LASER INTERFEROMETER GRAVITATIONAL WAVE OBSERVATORY
- LIGO -
CALIFORNIA INSTITUTE OF TECHNOLOGY
MASSACHUSETTS INSTITUTE OF TECHNOLOGY

Technical Note **LIGO-T960191-00 - D** December, 1996

Modal Model Update 5

Large Angle Regime

Daniel Sigg

Distribution of this draft:

ASC

This is an internal working note
of the LIGO Project.

California Institute of Technology
LIGO Project - MS 51-33
Pasadena CA 91125
Phone (818) 395-2129
Fax (818) 304-9834
E-mail: info@ligo.caltech.edu

Massachusetts Institute of Technology
LIGO Project - MS 20B-145
Cambridge, MA 01239
Phone (617) 253-4824
Fax (617) 253-7014
E-mail: info@ligo.mit.edu

WWW: http://www.ligo.caltech.edu/

1 ABSTRACT

This document reports the results of the modal model simulations extended to many modes and applied at large angular misalignments. Three main topic are investigated: the modal decomposition of the electric fields (section 3), the servo-stability of the length sensing signals (section 4) and the linearity of the wavefront sensing signals (section 5). The investigations are made along the axes which are diagonal for the degradation of the gravitational-wave readout [5].

Table 1 summarized the findings. Even so the angles for which the power in the recycling and the in-line arm cavity has dropped by factor of two and the stability boundaries for longitudinal and angular misalignments are vastly different in different directions, they are usually very similar in absolute values for each of the above effects. The smallest limit for a stable alignment is obtained for a misalignment in the direction of M5: $\sim 1 \times 10^{-7}$ rad. This misalignment involves only the recycling mirror and the ITMs, hence, suggesting that during lock acquisition the recycling cavity should be aligned before the arm cavities are brought into resonance.

Table 1: Power degradation and decrease of servo stability due to angular misalignments. For each principle angular direction the angle for which the power has degraded by half and the angle for which the length and alignment sensitivities have decreased by half are shown. The values are given in units of the arm cavity divergence angle.

Direction	Recycling cavity power		Power in arm	Stability (half gain point)	
	sidebands	carrier	carrier	LSC	ASC
M1	> 1	> 1	> 1	> 1	> 1
M2	0.7	0.6	0.5	0.6	0.65
M3	0.3	> 0.6	> 0.6	0.15	0.15
M4	0.15	0.06	0.06	0.04	0.04
M5	0.015	> 0.1	> 0.1	~0.01	~0.01

2 DEFINITIONS AND PARAMETERS

The basic principles of the simulation code (modal model) are derived in Ref. [1]. The necessary conventions and the interferometer equations are further outlined in Ref. [2]. The parameters used in the present simulations (see Table 2) are based on Ref. [3]. The effects of small misalignments are reported in Ref. [6] for angular misalignments and in Ref. [7] for mode/curvature mismatch and are not repeated here again.

In the present work angular degree of freedoms are expressed in the basis which is diagonal for the degradation of the gravitational-wave sensitivity at the dark port [5], called the M-basis. In Table 3 the basis vectors are listed in terms of the usual differential and common misalignments angles of the test masses. The results of present work were obtained by computing 21 transverse modes.

Table 2: Interferometer parameters. LIGO 4km configuration.

Parameter	Unit	arm (ITM)	arm (ETM)	recycl. (RM)
length (common / differential)	m		3999.01	9.38 / 0.21
power transmission	%	3	0.0015	2.44
power reflectivity	%	96.995	99.9935	97.5
radius of curvature	m	–14571	7400	–9998.65
modulation frequencies	MHz		23.971	35.956
modulation depths	Γ		0.45	0.045
wave length	μm			1.064
refractive index				1.44968

Table 3: Basis vectors for expressing large angular misalignments

Vector	angular degree of freedom				
	ΔETM	ΔITM	$\overline{ETM}$	$\overline{ITM}$	RM
M1	0.000	0.000	**0.392**	**–0.747**	**–0.537**
M2	0.000	0.000	**0.920**	**0.317**	**0.231**
M3	**–0.421**	**0.907**	0.000	0.000	0.000
M4	**0.907**	**0.421**	0.000	0.000	0.000
M5	0.000	0.000	–0.002	**–0.585**	**0.811**

3 Mode Decomposition for Large Angles

When an interferometer is misaligned higher order transverse modes are excited in the cavities. Generally, the number of significant modes and the amplitudes of these modes are increasing with larger and larger angles. Since it is numerically costly to compute the large number of necessary modes for large misalignments, we restrict the investigation to the angular degree of freedoms which were found to be diagonal for the degradation of the gravitational wave sensitivity (M-basis). The justification for this choice lies in the observation that more sensitive degree of freedoms for the gravitational wave sensitivity are also the more sensitive degree of freedoms for the degradation of the cavity power and the degradation of the length and alignment sensitivity matrices.

Table 1 summarizes the values of angles (in the M-basis) where the cavity power in the arms and in the recycling cavity have dropped by half compared to the power in the perfectly aligned case. In the recycling cavity the values are given for the carrier and the resonant sidebands separately. Because the sidebands are not resonant in the arm cavities, only the carrier values are listed. Fig. 1 shows the absolute electric field amplitudes as a function of the misalignment angle in the direction of M4 for the dark port of the Michelson, in reflection of the recycling cavity, inside the recycling cavity and inside one of the arm cavities. The input field is a pure TEM_{00} with amplitude 1 and the results are given for the lowest six modes in one transverse dimension: TEM_{00} through TEM_{50}. The plots include the lowest six modes for both carrier and sideband fields. The sign of the value for the carrier field is determined from the sign of its real part. From the second row in Fig. 1 one can then see that the carrier field in reflection has a zero crossing at ~0.35 and changes its sign; thus, going from an overcoupled system to an undercoupled one with increasing angular misalignment in the M4 direction.

4 Longitudinal Sensitivity at Large Angles

For the length sensing and control system to be able to servo the longitudinal degree of freedoms in the presence of a large angular misalignment, the measured error signals must still be a 'good' measure of the longitudinal deviations. For a single-input-single-output longitudinal servo system it is straight forward to define the ratio of sensitivities between the angular misaligned and aligned case as a criterion of stability. If this ratio is unity, the angular misalignment obviously does not interfere with the longitudinal degree of freedom and we say that the system is stable. If this ratio grows larger than unity, the longitudinal error signal is over-estimated and it is expected that the system is still able to find zero point of longitudinal deviation. If the ratio becomes smaller than unity, the servo loop gain will decrease, until, ultimately, for negative ratios the longitudinal error signal has the wrong sign and the system becomes unstable.

In the case of a multi-dimensional longitudinal servo system the situation is a little bit more complicated, since the longitudinal deviations are now related to the measured error signals via a matrix, called the length sensitivity matrix:

$$L_{ifo} \equiv \left.\frac{\partial \vec{S}_{err}}{\partial(\overrightarrow{\Delta L})}\right|_{ifo} \tag{1}$$

where $\vec{S}_{err}$ denotes the measured error signals and $\overrightarrow{\Delta L}$ denotes the longitudinal deviations. For small deviations in length the error signals are then obtained by:

$$\vec{S}_{err} = L_{ifo}\overrightarrow{\Delta L} \tag{2}$$

Going from the perfectly aligned state to state with large angular misalignment, the length sensitivity matrix will change. Since it is a matrix the change might be more complicated than a simple 'gain' reduction, the decrease (or increase) of sensitivity can happen differently for each longitudinal degree of freedom. Furthermore, the matrix might undergo a rotation. It is therefore not possible to just look at individual degree of freedoms separately, but rather one has to define a new stability criterion which gives a measure how well the measured longitudinal error signals represent the true deviations in length. If one defines LSM as the length sensitivity matrix for the perfectly aligned interferometer, one can obtain an estimation of the deviations in length for an interferometer in an 'unknown state' as follows:

$$\overrightarrow{\Delta L}' = \mathrm{LSM}^{-1}\vec{S}_{err} = \mathrm{LSM}^{-1}L_{ifo}\overrightarrow{\Delta L} \tag{3}$$

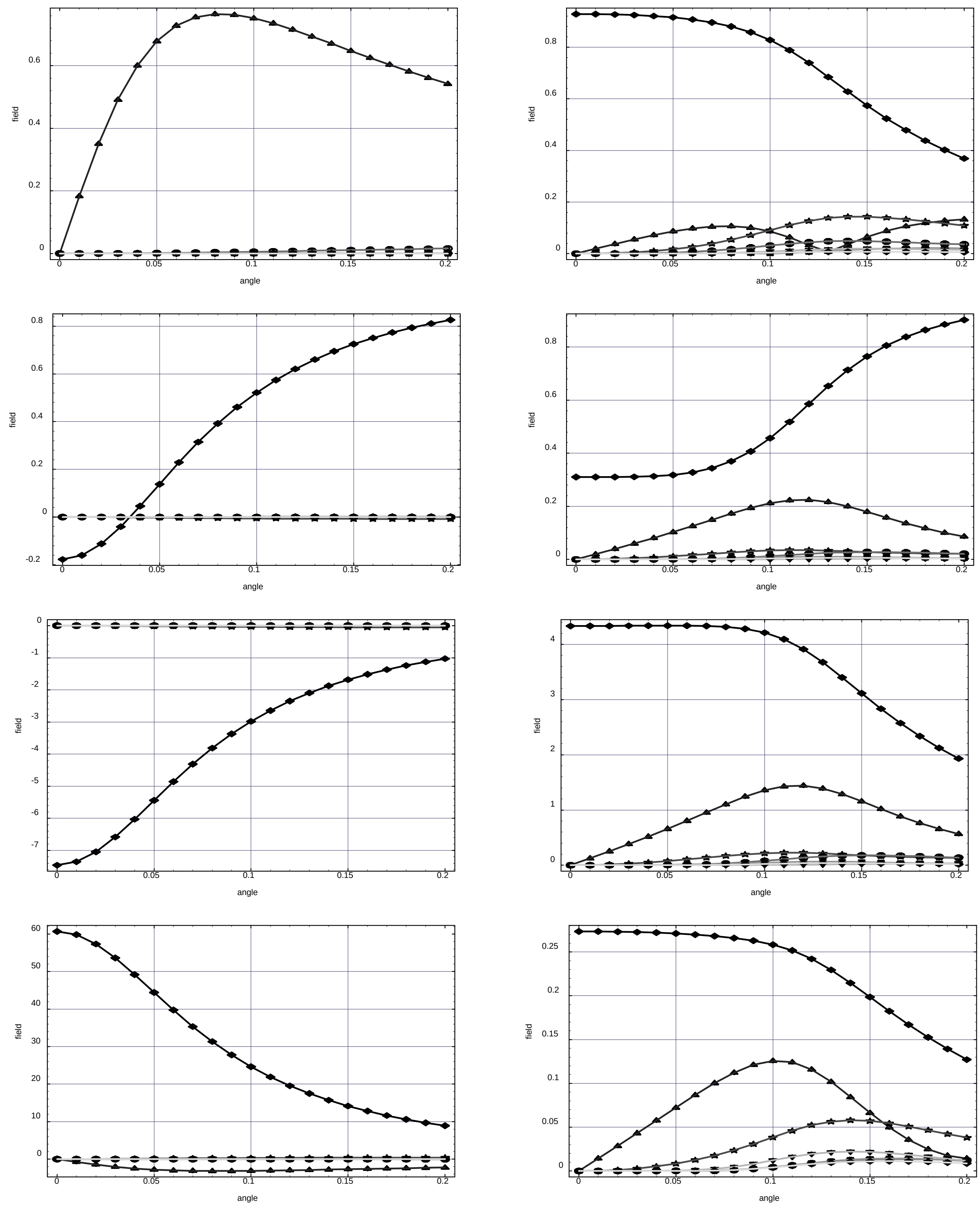

Figure 1: Electric field amplitudes. The fields are plotted as a function of the misalignment angle in the direction of M4 for both carrier (first column) and sidebands. The following points are used: at the dark part (first roe), in reflection, inside the recycling cavity and inside the in-line arm cavity (last row). The angles are given in units of the arm cavity divergence angle. The plot points for increasing mode order are: diamond, triangle (up), star, circle, square and triangle.

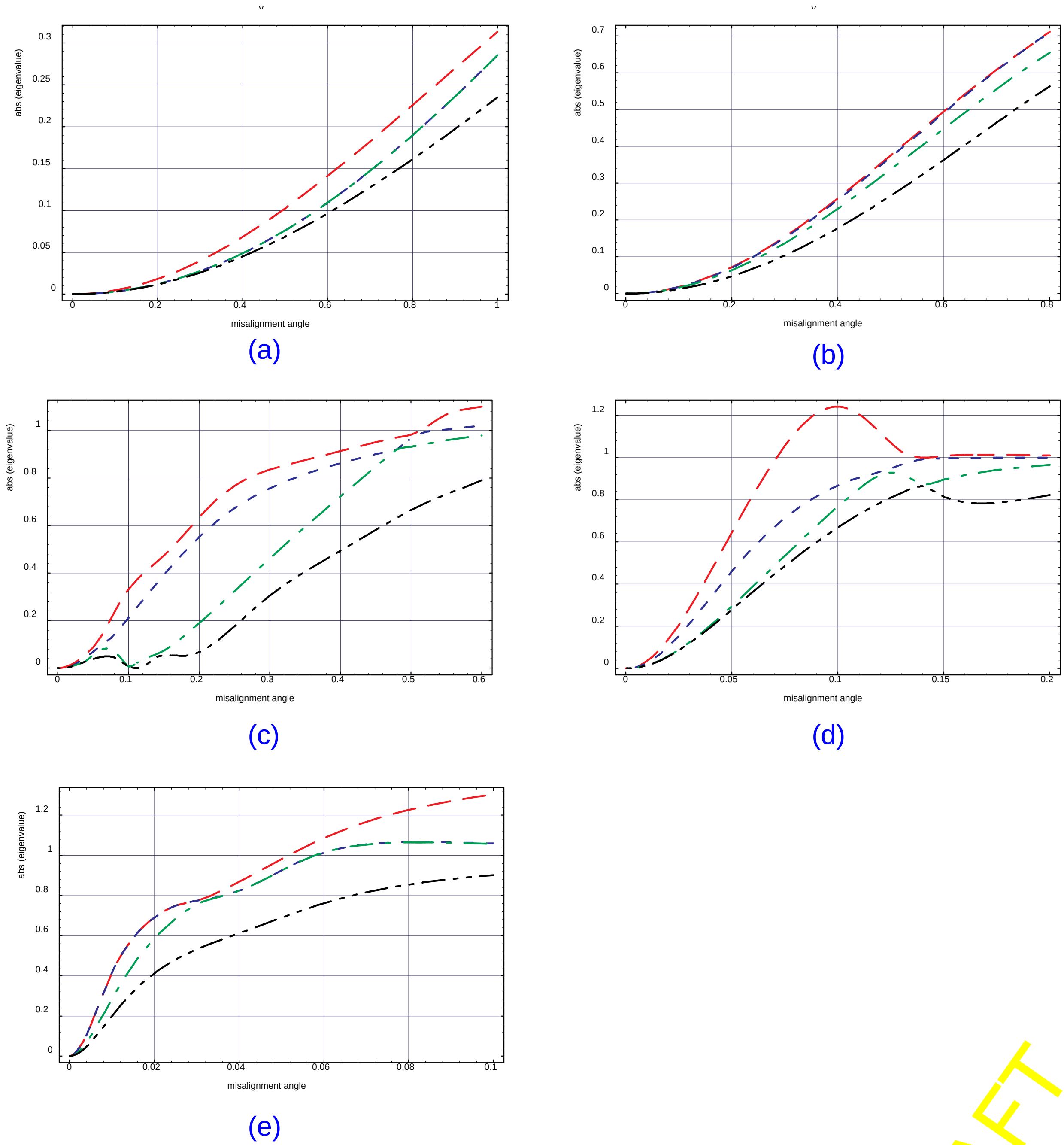

Figure 2: Stability Criterion for Length Sensing. The absolute values of the eigenvalues of the length sensing convergence matrix are shown for misalignments in the direction of M1 (a) through M5 (e). Small values indicate a good behavior of the length sensitivity matrix, whereas for values above unity longitudinal error signals may have the wrong sign (for details see text). The misalignment angles are given in units of the divergence angle.

We can then define a stability criterion by demanding that the difference between the estimated deviation in length and the true one is smaller than the deviation itself, i.e.:

$$\langle\overrightarrow{\Delta L}' - \overrightarrow{\Delta L}|\overrightarrow{\Delta L}' - \overrightarrow{\Delta L}\rangle < \langle\overrightarrow{\Delta L}|\overrightarrow{\Delta L}\rangle \text{ for all small } \overrightarrow{\Delta L}\,. \tag{4}$$

Using Eqn. (3) in (4) gives:

$$\langle\overrightarrow{\Delta L}|(\mathbf{1} - \mathrm{LSM}^{-1}L_{ifo})^2|\overrightarrow{\Delta L}\rangle < \langle\overrightarrow{\Delta L}|\overrightarrow{\Delta L}\rangle \tag{5}$$

where **1** is the identity matrix.

Because Eqn. (5) must be valid for all small deviations in length $\overrightarrow{\Delta L}$, one can formulate the condition (4) independent of the deviations in length by looking at the eigenvalues of the operator in the bra-ket. By defining the convergence matrix as

$$C_L = \mathbf{1} - \mathrm{LSM}^{-1}L_{ifo} \tag{6}$$

all its eigenvalues must lie inside the unity circle in order for the length sensitivity matrix L_{ifo} to be called stable, i.e.

$$\max|\text{eigenvalues } C_L| < 1 \tag{7}$$

Alternatively, one could formulate a weaker condition and only ask that $\overrightarrow{\Delta L}$ and $\overrightarrow{\Delta L}'$ point 'overall' in the same direction.

$$\langle\overrightarrow{\Delta L}|\overrightarrow{\Delta L}'\rangle > 0 \text{ and thus } \langle\overrightarrow{\Delta L}|\mathrm{LSM}^{-1}L_{ifo}|\overrightarrow{\Delta L}\rangle > 0 \tag{8}$$

This condition can again be expressed as an eigenvalue equation:

$$\mathrm{Re}\{\text{eigenvalues } (\mathrm{LSM}^{-1}L_{ifo})\} > 0 \tag{9}$$

For most cases of misaligned interferometers Eqns. (7) and (9) give the same stability boundary, since the boundary is mostly determined by a 'sign-flip' in the length sensitivity matrix and not by an excessive increase of 'gain'. Fig. 2 shows the absolute values for the eigenvalues of the convergence matrix as a function of an angular misalignment in the directions of M1 to M5. Table 1 summarizes the angular values where the first eigenvalue of the convergence matrix exceeds 0.5 and therefore indicating a gain loss of about 0.5.

5 Wavefront Sensing at Large Angles

Similarly to the longitudinal degree of freedoms, one can ask whether the measured wavefront sensing signals are still a good measure of the physical misalignment angles assuming one would make a large angular misalignment, but would not know the exact alignment state of the interferometer. Since the present work only investigates misalignments along the axes of the M basis, a stability criterion can be written as:

$$C_{WFS} = \frac{\langle\overrightarrow{\Delta\Theta}' - \overrightarrow{\Delta\Theta}|\overrightarrow{\Delta\Theta}' - \overrightarrow{\Delta\Theta}\rangle}{\langle\overrightarrow{\Delta\Theta}|\overrightarrow{\Delta\Theta}\rangle} < 1 \tag{10}$$

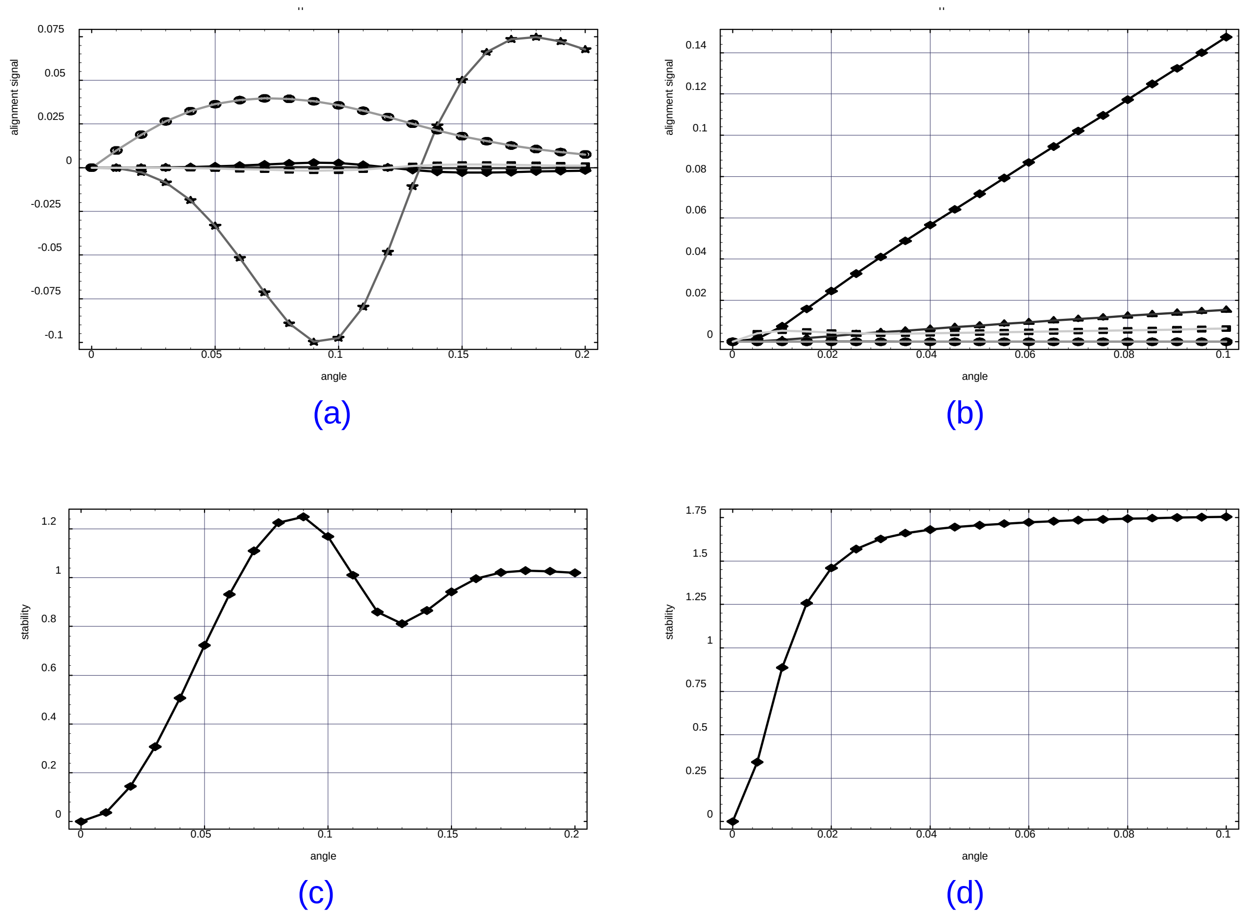

Figure 3: Alignment Signals and Stability Criterion. The estimated misalignment angles are plotted against the physical ones (first row) in units of the arm cavity divergence angle and in the direction of M4 (first column) and M5. Diamonds, triangles, stars, circles and squares are used to denote basis vectors M1 through M5. The second row shows the stability criterion for the wavefront sensing scheme (see text for details).

where $\overrightarrow{\Delta\Theta}$ is the physical misalignment angle and $\overrightarrow{\Delta\Theta}'$ is its estimation using the alignment sensitivity matrix of the perfectly aligned interferometer (ASM),

$$\overrightarrow{\Delta\Theta}' = \mathrm{ASM}^{-1}\overrightarrow{WFS} \tag{11}$$

where $\overrightarrow{WFS}$ denotes the measured error signal of the wavefront sensors.

Fig. 3 shows the estimated misalignment angles as function of the physical ones when the interferometer is misaligned in the directions of M4 or M5. Additionally, the stability criterion C_{WFS} is computed along these axis. M4 and M5 are the two degree of freedoms which are most sensitive to angular misalignments. The corresponding figures for the M1 to M3 are generally showing weaker dependencies and fewer ambiguities. Table 1 summarizes the angular values where the stability criterion exceeds 0.5 and thus indicating a gain loss of about 0.5.

REFERENCE

[1] Y. Hefetz, N. Mavalvala and D. Sigg, *"Principles of calculating alignment signals in complex optical interferometers"*, LIGO-P960024-A-D (1996).

[2] D. Sigg, *"Modal model update 1: Interferometer operators"*, LIGO-T960113-00-D (1996).

[3] D. Shoemaker, *"Detector Subsystem Requirements"*, LIGO-E960112-05-D (1996).

[4] D. Sigg, *"Wavefront sensor"*, LIGO-T960111-A-D (1996).

[5] D. Sigg, *"Modal model update 2: GW-sensitivity to angular misalignments"*, LIGO-T960114-B-D (1996).

[6] D. Sigg, *"Modal model update 3: Small angle regime"*, LIGO-T960115-A-D (1996).

[7] D. Sigg, *"Modal model update 4: Mode Mismatch"*, LIGO-T960116-00-D (1996).